



**Topological Modulation of Porous Structure of Coordination Polymer Constructed with Flexible Building Block via Framework-Guest Interaction during Self-Assembly**

Journal:	<i>CrystEngComm</i>
Manuscript ID	CE-COM-09-2015-001804.R2
Article Type:	Communication
Date Submitted by the Author:	26-Dec-2015
Complete List of Authors:	Masuya-Suzuki, Atsuko; Tohoku University, Grad. Sch. Environm. Studies Matsubara, Nozomi; Tohoku University, Grad. Sch. Environm. Studies Karashimada, Ryunosuke; Tohoku University, Grad. Sch. Environm. Studies Hoshino, Hitoshi; Tohoku University, Grad. Sch. Environm. Studies Iki, Nobuhiko; Tohoku University, Grad. Sch. Environm. Studies

Topological Modulation of Porous Structure of Coordination Polymer Constructed with Flexible Building Block via Framework-Guest Interaction during Self-Assembly

Atsuko Masuya-Suzuki,\* Nozomi Matsubara, Ryunosuke Karashimada, Hitoshi Hoshino, and Nobuhiko Iki\*

Graduate School of Environmental Studies, Tohoku University, 6-6-07 Aramaki-aza Aoba, Aoba-ku, Sendai, Miyagi 980-8579, Japan

\* To whom correspondence should be addressed. Fax: +81-22-795-7293, Email: masuya@analchem.che.tohoku.ac.jp, iki@m.tohoku.ac.jp

**Abstract**

Porous structure of a coordination polymer constructed with a Sm(III) ion and a conformationally flexible ligand is modulated by guest solvents. The coordination polymer containing guest DMF possesses isolated hydrophobic and hydrophilic voids, while the one containing guest methanol has a microchannel with alternately arranged hydrophobic–hydrophilic surfaces.

Coordination polymers have attracted considerable attention for various applications such as in adsorption or separation in gas<sup>1</sup> and liquid phases,<sup>2</sup> as heterogeneous catalysts<sup>3</sup> and luminescent materials,<sup>4</sup> and for molecular recognition,<sup>5</sup> due to their intrinsic physicochemical properties. So far, most studies in this research field have employed geometrically rigid ligands with d-block metal ions. The self-assembly during crystal growth is programmed by strong and directionally defined metal-ligand bonding and hydrogen bond, and this approach has successfully provided a range of functional materials.<sup>6</sup> On the other hand, the use of conformationally flexible ligands and trivalent lanthanide (Ln(III)) ions is expected to yield a unique topology and properties that are hard to be obtained from the rigid building blocks.<sup>7</sup> However, because of the molecular flexibility of the ligand and flexible coordination geometry of the Ln(III) ions, the prediction of the topology is often difficult. Further, even a slight difference in the reaction condition would result in considerable structural changes of the framework. This is because weaker intermolecular interactions such as CH $\cdots$ O, CH $\cdots$ N, and CH $\cdots$  $\pi$  hydrogen bonds,  $\pi$ - $\pi$  interactions, and halogen bonds can significantly affect the self-assembly process. In the design of novel functional materials, it is a challenging and vital task to understand how the synthetic conditions affect the overall network of the Ln(III) coordination polymer with conformationally flexible ligands. In particular, a guest solvent can be a crucial factor that determines the framework topology of coordination polymers as a template for crystal growth.<sup>8</sup> Such template effects on the self-assembly of flexible ligands and Ln(III) ions are much less explored than those of rigid ligands and d-block metal ions.

In our previous study, as a conformationally flexible ligand, we focused our attention on

a tripodal Schiff base,<sup>9</sup> which is known to adopt diverse coordination modes for discrete Ln(III) complexes.<sup>10</sup> We prepared a novel Ln(III) coordination polymer based on the Schiff base ( $H_3L$ , Fig. 1) and showed that the formation of the coordination polymer was attributable to factors such as coordination of the Schiff base in the proton-undissociated form  $H_3L$ , coordination of nitrate anions, and electron-donating substituents at the *para*-position to the hydroxyl groups of the Schiff base.<sup>11</sup> Herein, we show that the interaction between the framework and the guest solvents has a significant impact on the topology of the porous structure of the Ln(III) coordination polymer.

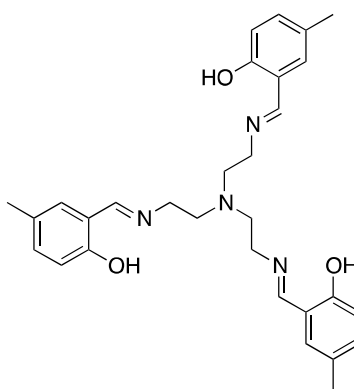


Fig. 1 Chemical structure of a tripodal Schiff base ligand ( $H_3L$ ) prepared by condensation of tris(2-aminoethyl)amine with 5-methylsalicylaldehyde.

The coordination polymer  $[\text{Sm}(\text{H}_3\text{L})(\text{NO}_3)_3 \cdot \text{DMF} \cdot 1/6\text{H}_2\text{O}]_n$  (**1**, DMF = *N,N*-dimethylformamide) was obtained by the one-pot condensation of 5-methylsalicylaldehyde with tris(2-aminoethyl)amine in the presence of  $\text{Sm}(\text{NO}_3)_3 \cdot 6\text{H}_2\text{O}$  and recrystallization from DMF. The compound **1** crystallizes in the rhombohedral space group  $R\bar{3}$  with 18 formula units per unit cell. As shown in Fig. S1a, the asymmetric unit of **1** consists of three nitrate anions, a Sm(III) ion, a  $\text{H}_3\text{L}$ , a DMF, and 1/6 water. The solvent molecules do not coordinate to the Sm(III) ion, but are only present as guest molecules. The Sm(III) center is coordinated to nine oxygen atoms, i.e., six oxygen atoms from three nitrates and three phenol oxygen atoms from three different  $\text{H}_3\text{L}$  ligands. The  $\text{Sm}(\text{NO}_3)_3$  units are connected with  $\text{H}_3\text{L}$  to form a 3D structure (Fig. S1b) containing two types of voids: one is hydrophobic, and the other is hydrophilic. The hydrophobic wall is composed of methyl groups of  $\text{H}_3\text{L}$  (Fig. 2a), and no guest molecules are included in this void. The hydrophilic wall is composed of nitrate oxygen atoms and methylene groups of  $\text{H}_3\text{L}$  (Figs. 2b and 2c), and this void contains a water molecule and DMF molecules as guest molecules. The spatial arrangement of these voids in the unit cell is shown in Figs. 3a and 3b. As can be seen in Fig. 3b, the hydrophobic and hydrophilic voids appear alternately along the *c* axis. When the guest water and DMF molecules are removed, the total solvent-accessible void volume per unit cell is  $3272.2 \text{ \AA}^3$  (estimated with standard van der Waals radii and a  $1.2 \text{ \AA}$  probe radius), which represents 18.2 % of the unit cell volume.

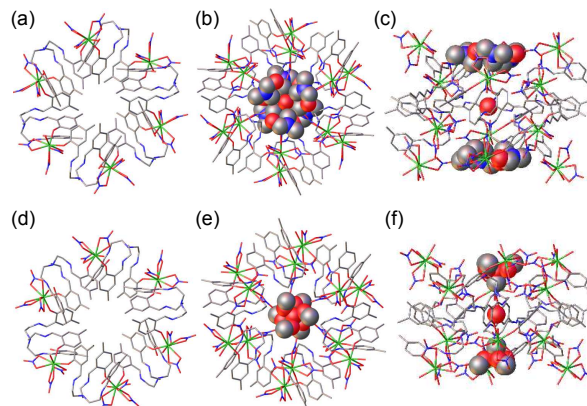


Fig. 2 Structures of  $[\text{Sm}(\text{H}_3\text{L})(\text{NO}_3)_3 \cdot \text{DMF} \cdot 1/6\text{H}_2\text{O}]_n$  (**1**) and  $[\text{Sm}(\text{H}_3\text{L})(\text{NO}_3)_3 \cdot 1/3\text{MeOH} \cdot 1/6\text{H}_2\text{O}]_n$  (**2**). (a) View along the  $c$  axis of the hydrophobic void in **1**. (b) View along the  $c$  axis of the hydrophilic void in **1**. (c) View along the  $a$  axis of the hydrophilic void in **1**. (d) View along the  $c$  axis of the hydrophobic void in **2**. (e) View along the  $c$  axis of the hydrophilic void in **2**. (f) View along the  $a$  axis of the hydrophilic void in **2**. C: gray, O: red, N: blue, Sm: green. Guest solvents are shown with space-filling model. All hydrogen atoms and disorders in  $\text{H}_3\text{L}$  and nitrate anions are omitted for clarity.

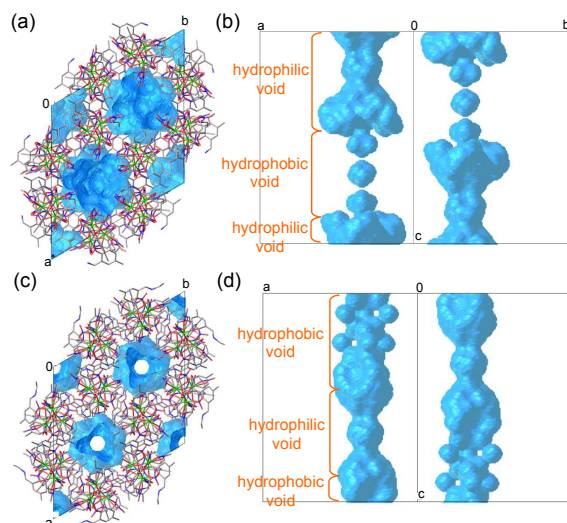


Fig. 3 Spatial arrangements of the hydrophobic and hydrophilic voids in the unit cells of  $[\text{Sm}(\text{H}_3\text{L})(\text{NO}_3)_3 \cdot \text{DMF} \cdot 1/6\text{H}_2\text{O}]_n$  (**1**) and  $[\text{Sm}(\text{H}_3\text{L})(\text{NO}_3)_3 \cdot 1/3\text{MeOH} \cdot 1/6\text{H}_2\text{O}]_n$  (**2**). Void surface is shown in light blue. View along the  $c$  axis in **1** (a) and in **2** (c). View along  $[110]$  in **1** (b) and in **2** (d).

A slight change in the crystallization method of **1**, namely, slow vapor diffusion of methanol into the DMF solution yields  $[\text{Sm}(\text{H}_3\text{L})(\text{NO}_3)_3 \cdot 1/3\text{MeOH} \cdot 1/6\text{H}_2\text{O}]_n$  (**2**, MeOH = methanol). The coordination polymer **2** crystallizes in the rhombohedral space group  $R\bar{3}$  and the asymmetric unit consists of three nitrate anions, a Sm(III) ion, a  $\text{H}_3\text{L}$ ,  $1/3$  MeOH, and  $1/6$  water molecules (Fig. S2). The compound **2** also has a hydrophobic void (Fig. 2d) and a hydrophilic void containing a guest water and methanol molecule (Fig. 2e and f). Despite similarities between the asymmetric unit of **1** and that of **2**, the guest molecule has a significant impact on the topological modulation of the porous structure of the coordination polymer. For instance, the diameters of the hydrophobic and hydrophilic voids of **2** (Fig. 3d) are more homogeneous than those of **1** (Fig. 3b), resulting in a microchannel with alternately arranged hydrophobic–hydrophilic surfaces along the  $c$  axis. To the best of our knowledge, a coordination polymer with such a pore consisting of hydrophobic and hydrophilic region is unprecedented, although coordination polymers having both hydrophobic and hydrophilic pores have been reported.<sup>12</sup> When the guest water and methanol molecules are removed, the total solvent-accessible void volume per unit cell is  $2587.2 \text{ \AA}^3$ , which represents 15.0 % of the unit cell volume.

The topological difference between the porous structures of **1** and **2** seems to be caused by the template effect of the guest solvent. In the structure of **1**, the guest DMF molecules are located without site disorder in a pocket between the hydrophobic and hydrophilic voids (Figs. 4a-c). There are  $\text{CH}\cdots\text{O}$  hydrogen bonds between the framework and DMF. Herein, we use a  $\text{H}\cdots\text{O}$  distance cut-off of  $3.0 \text{ \AA}$ , which is larger than the sum of the van der Waals radii, since the weak  $\text{CH}\cdots\text{O}$  hydrogen bond can be distorted easily



by crystal packing.<sup>13</sup> The CH $\cdots$ O hydrogen bonds from the framework to the oxygen atom of DMF, and ones from DMF to the nitrate oxygen of the framework are observed in **1** (Fig. 4d, Table S1). Additionally, as shown in Fig. S3, the DMF molecules are weakly connected to each other by CH $\cdots$ O hydrogen bonds (Table S1). A total of nine cooperative CH $\cdots$ O hydrogen bonds per one DMF molecule supports the unique location of the DMF molecule in the pocket. These framework-guest interactions should contribute to defining the topology of **1**. In the self-assembly process, the preformed coordination macrocycles would interact with the solvent molecules by CH $\cdots$ O hydrogen bonds, and then the framework would be constructed.

By contrast, the methanol molecules in **2** are located in the central space of the hydrophilic pore with site disorder (Figs. 4e-g). The methyl group of the methanol molecule forms three symmetrical CH $\cdots$ O hydrogen bonds to the nitrate oxygen atoms of the framework (Figs. 4h and S4). The number of the CH $\cdots$ O hydrogen bonds per molecule is smaller than that of DMF due to the poor structural fitting of the methanol molecule toward the framework as compared to DMF. Notably, as shown in Fig. S5, the space corresponding to the pocket observed in **1** is packed by the methyl group of H<sub>3</sub>L and the nitrate anion, and cannot be accessed by the solvent in **2**. Thus, the hydrophilic region of **2** is contracted as compared to **1**. Furthermore, the guest-free hydrophobic region is also influenced by the solvent. As can be seen in Fig. S6, the guest-free hydrophobic void is surrounded by the guest-containing hydrophilic voids in the *ab* plane. Therefore, the contraction of the hydrophilic region in **2** leads to the expansion of the hydrophobic region in **1**. These observations strongly suggest that the guest solvents can significantly

influence the topology of the porous structure of the Sm(III) coordination polymer as a template during the self-assembly.

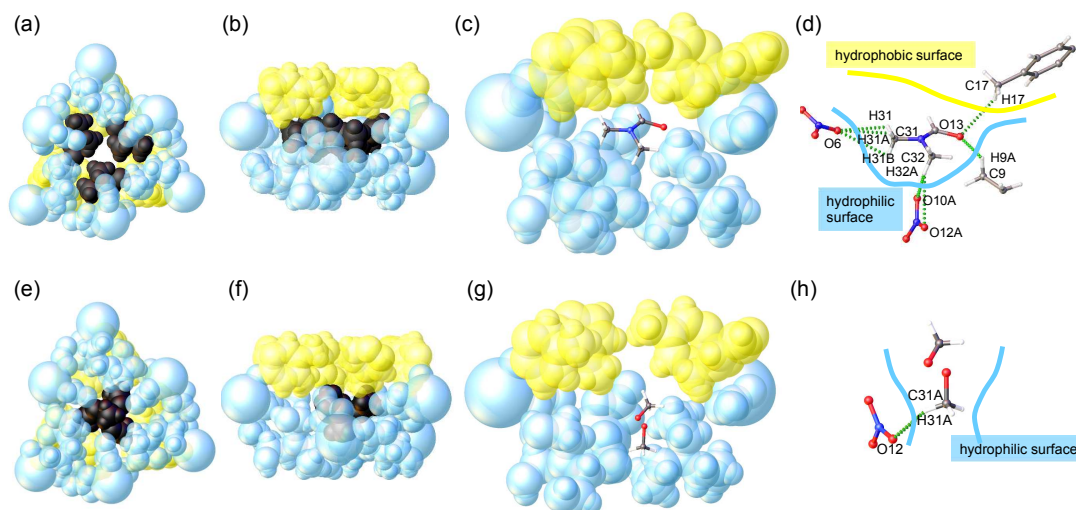


Fig. 4 Environments of the guest molecules in **1** and **2**. (a) View along the *c* axis for the DMF-containing void in **1** and (b) view along the *a* axis for the DMF-containing void in **1**; the hydrophobic surface is shown in yellow, the hydrophilic surface is shown in pale blue, the guest DMF molecules are shown in black. (c) Depiction of the pocket surrounding the guest DMF molecule in **1** and (d) the CH...O interactions between the framework and the guest DMF molecule in **1**. (e) View along the *c* axis for the methanol-containing void in **2** and (f) view along the *a* axis for the methanol-containing void in **2**; the methanol molecules are shown in black. (g) Depiction of the guest methanol in **2** and (h) the CH...O interactions between the framework and the guest methanol molecule in **2**.

Significant conformational difference of the Schiff base is observed between **1** and **2**. As illustrated in Fig. S7, the C1–C2–C3–C4–C5–C6 aromatic ring and N1–H1–O1–C2–C1–C8 ring are coplanar owing to the support of the hydrogen bond; therefore, the conformational flexibility of the ligand is mainly based on the twisting of the arms along

the N4–C10, C10–C9, and C9–N1 bonds. Similarly, the remaining two arms can twist along the N4–C20, C20–C19, and C19–N2, and N4–C30, C30–C29, and C29–N3 bonds, respectively. The torsion angles of the Schiff base in **1** and **2** are summarized in Table 1, and significant differences of at most 10° are observed on comparing the angles of **1** and **2**. As summarized in Table S2, the Sm–O bond lengths of **1** agree well with those of **2**, while the selected bond angles of **1** listed in Table S3 differ considerably from those of **2**. These observations suggest that the change in the conformation of the Schiff base and the coordination geometry of the Sm(III) ions allow the topological change of the framework.

Table 1. Torsion angles (deg) of **1** and **2**.

	<b>1</b>	<b>2</b>
C9–C10–N4–C20	78.1(7)	83.3(6)
N1–C9–C10–N4	73.3(8)	71.4(6)
C8–N1–C9–C10	104(1)	107.8(6)
C19–C20–N4–C30	81.0(8)	78.5(7)
N2–C19–C20–N4	72.1(11)	65.7(6)
C18–N2–C19–C20	123(1)	121.3(6)
C29–C30–N4–C10	84.6(8)	81.4(6)
N3–C29–C30–N4	70.8(8)	73.9(6)
C28–N3–C29–C30	123.4(8)	133.5(6)

In order to see thermal properties of the compounds **1** and **2**, thermogravimetric analyses (TGA) were carried out. The TGA curve of **1** (Fig. S8a black line) shows a weight loss of 7.55 % from 60 to 220 °C, which corresponds to the loss of one DMF molecule and 1/6 water molecule per formula unit (calcd: 8.33 %). Then the framework begins to collapse at around 250 °C. The TGA curve of **1** which was measured after heating of the sample at 120 °C (Fig. S8a red line) also shows the decomposition of the

framework above 250 °C, indicating that the water and DMF molecules are successfully removed without the collapse of the framework. The TGA curve of the as-synthesized **2** (Fig. S8b black line) shows a weight loss of 1.92 % from 60 to 160 °C, which corresponds to the loss of 1/3 methanol and 1/6 water molecules (calcd: 1.61 %). Then the framework starts to decompose at around 250 °C. The TGA curve of **2** which was measured after heating of the sample at 80 °C (Fig. S8b red line) shows the similar thermal stability of the framework as that of the as-synthesized **2**, indicating that the solvent molecules are successfully removed without the collapse of the framework.

In order to check the phase purity, powder X-ray diffraction (PXRD) patterns were measured on the compounds **1** and **2** at room temperature. Each PXRD pattern (Fig. S9 blue line) agrees well with the theoretical peak pattern (Fig. S9 black line) obtained using the program Crystal Diffract and the single crystal structural data. These results confirm the purity of each sample. After the as-synthesized powders of **1** and **2** were heated to 200, 220 and 240 °C, the PXRD patterns (Fig. S9 red, green and orange lines, respectively) suggest that the framework is maintained up to 240 °C. Interestingly, in the PXRD patterns, there is a shift of the 11-3 reflection from 10.80° for the as-synthesized **1** (Fig. S9a blue line) to 11.16° for heated **2** at 240 °C (Fig. S9a orange line). The slight shift for heated **2** is also observed from 11.02° (Fig. S9b blue line) to 11.18° (Fig. S9b orange line). These observations indicate that the removal of the guest solvents induces the structural change in the framework. After further thermal treatment, the PXRD patterns show that the compounds **1** and **2** lose their crystalline natures at 270 °C (Fig. S9 pale blue line).

The N<sub>2</sub> adsorption of the compounds **1** and **2** at 77 K was measured after removal of

the solvents by heating at 120 °C under reduced pressure. As shown in Fig. S10, adsorption isotherms of the two compounds show sudden increase around  $P/P_0 = 0.7$  and desorption branches show large hysteresis. It is known that flexible coordination polymers show gate-opening effect, in which structural transformation from closed to open form occurs at a certain pressure.<sup>14</sup> Thus the observed adsorption behavior of **1** and **2** may correspond to this gate-opening phenomena. Combined with the results of PXRD measurements discussed above, the compounds **1** and **2** appear to be closed form after the removal of the solvents. The sudden change of the adsorption suggests that the structural transformation from the closed form to the open one at  $P/P_0 = 0.7$  due to the flexibility of the framework. In the desorption branch, the compounds **1** and **2** show the large hysteresis, indicating the strong affinity of N<sub>2</sub> molecules to the open structure. Based on the above interpretation, the total pore volume of **1** in the open form was estimated to be 0.073 cm<sup>3</sup> g<sup>-1</sup> and that of **2** was estimated to be meaningfully smaller value 0.060 cm<sup>3</sup> g<sup>-1</sup>. The open structures of **1** and **2** should be nearly same structures as the as-synthesized **1** and **2** (Fig. 3), respectively. Indeed, by deleting the crystal solvents from the crystal structures, the pore volume of the as-synthesized compound was estimated to be 0.120 cm<sup>3</sup> g<sup>-1</sup> for **1** and 0.102 cm<sup>3</sup> g<sup>-1</sup> for **2**. These values are in fair agreement with those determined by the N<sub>2</sub> adsorption in their magnitude and difference between **1** and **2**. Consequently, the N<sub>2</sub> adsorption result is consistent with our finding that the topology of the Sm(III) coordination polymer constructed with the conformationally flexible ligand can be modulated by the framework-guest interactions during the crystallization process.

## Conclusion

In this work, we have shown that the control over the topology of the porous structure of the Sm(III) coordination polymer constructed with the flexible ligand can be achieved by manipulating the framework-guest interaction during crystal growth. Different solvent species employed in the synthesis yield **1** and **2**, which possess different topology of the porous structure: **1** has isolated hydrophobic and hydrophilic voids, while **2** has an unprecedented microchannel with alternately arranged hydrophobic and hydrophilic surfaces. The guest DMF molecule in **1** is bound to a pocket of the framework by multiple CH $\cdots$ O hydrogen bonds. The guest methanol molecule in **2** is weakly bound to the framework due to the poor structural fitting to the framework. The combined effect of the conformational flexibility of the ligand and the flexible coordination geometry of the Sm(III) ion allows the topological modulation of the porous structure by the framework-guest interaction and yields an unusual pore surface arrangement. The TGA and PXRD results indicate that the guest molecules of **1** and **2** can be removed without the collapse of the frameworks. The N<sub>2</sub> adsorption shows the gate-opening effect due to the flexibility of the framework. The pore volume of **1** in the open form determined by N<sub>2</sub> adsorption is meaningfully larger than that of **2**. This observation supports our finding that the topology of the Sm(III) coordination polymer constructed with the conformationally flexible ligand can be modulated by the framework-guest interactions during the crystallization process.

## Acknowledgement

We thank Prof. T. Yoshioka (Graduate School of Environmental Studies, Tohoku University) and Assoc. Prof. T. Kameda (Graduate School of Environmental Studies, Tohoku University) for PXRD and TGA measurements. We thank Prof. T. Sato (IMRAM, Tohoku University) and Assoc. Prof. S. Yin (IMRAM, Tohoku University) for N<sub>2</sub> adsorption measurement.

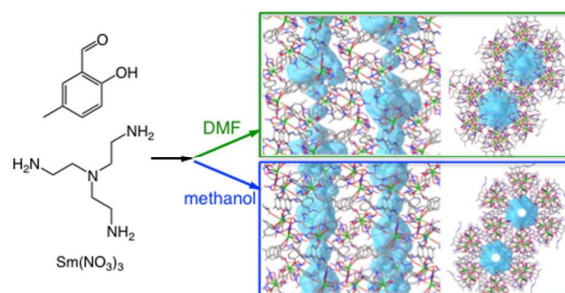
Electronic Supporting Information (ESI) available. CCDC 1405466 and 1405472 for compounds **1** and **2**. Experimental details, supplementary figures of crystallographic data, TGA profiles, experimental and simulated PXRD patterns, N<sub>2</sub> adsorption isotherms, and tables for X-ray crystallographic data, hydrogen-bond geometry, bond distances and angles. X-ray crystallographic CIF format.

## References

1. (a) J. -R. Li, R. J. Kuppler, H. -C. Zhou, *Chem. Soc. Rev.*, 2009, **38**, 1477. (b) B. Li, H. Wang, B. Chen, *Chem. Asian. J.*, 2014, **9**, 1474. (c) E. Barea, C. Montoro, J. A. R. Navarro, *Chem. Soc. Rev.*, 2014, **43**, 5419.
2. (a) Z. -Y. Gu, C. -X. Yang, N. Chang, X. -P. Yan, *Acc. Chem. Res.*, 2012, **45**, 734. (b) B. Van der Voorde, B. Bueken, J. Denayer, D. De Vos, *Chem. Soc. Rev.*, 2014, **43**, 5766.
3. J. Liu, L. Chen, H. Cui, J. Zhang, L. Zhang, C. -Y. Su, *Chem. Soc. Rev.*, 2014, **43**, 6011.
4. (a) Y. Cui, B. Chen, G. Qian, *Coord. Chem. Rev.*, 2014, **273-274**, 76. (b) L. V. Meyer, F. Schönfeld, K. Müller-Buschbaum, *Chem. Commun*, 2014, **50**, 8093. (c) Y. Wang, J. Yang, Y. -Y. Liu, J. -F. Ma, *Chem. Eur. J.* 2013, **19**, 14591.
5. B. Chen, S. Xiang, G. Qian, *Acc. Chem. Res.*, 2010, **43**, 1115.
6. (a) D. Zhao, D. J. Timmons, D. Yuan, H. -C. Zhou, *Acc. Chem. Res.*, 2011, **44**, 123. (b) W. Lu, Z. Wei, Z. -Y. Gu, T. -F. Liu, J. Park, J. Park, J. Tian, M. Zhang, Q. Zhang, T.

- Gentle III, M. Bosch, H. -C. Zhou, *Chem. Soc. Rev.*, 2014, **43**, 5561. (c) V. Guillermin, D. Kim, J. F. Eubank, R. Luebke, X. Liu, K. Adil, M. S. Lah, M. Eddaoudi, *Chem. Soc. Rev.*, 2014, **43**, 6141.
7. (a) F. C. Pigge, *CrystEngComm*, 2011, **13**, 1733. (b) Y. -P. He, Y. -X. Tan, J. Zhang, *J. Mater. Chem. C*, 2014, **2**, 4436.
8. Z. Zhang, M. J. Zaworotko, *Chem. Soc. Rev.*, 2014, **43**, 5444.
9. J. R. Broomhead, D. J. Robinson, *Aust. J. Chem.*, 1968, **21**, 1365.
10. (a) A. Smith, S. J. Rettig, C. Orvig, *Inorg. Chem.*, 1988, **27**, 3929. (b) D. J. Berg, S. J. Rettig, C. Orvig, *J. Am. Chem. Soc.*, 1991, **113**, 2528. (c) S. Liu, L. Gelmini, S. J. Rettig, R. C. Thompson, C. Orvig, *J. Am. Chem. Soc.*, 1992, **114**, 6081. (d) S. Liu, L. -W. Yang, S. J. Rettig, C. Orvig, *Inorg. Chem.*, 1993, **32**, 2773. (e) M. Kanesato, T. Yokoyama, O. Itabashi, T. M. Suzuki, M. Shiro, *Bull. Chem. Soc. Jpn.*, 1996, **69**, 1297. (f) M. Kanesato, T. Yokoyama, *Chem. Lett.*, 1999, 137. (g) S. Mizukami, H. Houjou, M. Kanesato, K. Hiratani, *Chem. Eur. J.*, 2003, **9**, 1521. (h) M. Kanesato, K. Nagahara, K. Igarashi, K. Sato, Y. Kikkawa, *Inorg. Chim. Acta*, 2011, **367**, 225.
11. A. Masuya, C. Igarashi, M. Kanesato, H. Hoshino, N. Iki, *Polyhedron*, 2015, **85**, 76.
12. (a) A. Kondo, H. Kajiro, H. Noguchi, L. Carlucci, D. M. Proserpio, G. Ciani, K. Kato, M. Tanaka, H. Seki, M. Sakamoto, Y. Hattori, F. Okino, K. Maeda, T. Ohba, K. Kaneko, H. Kanoh, *J. Am. Chem. Soc.*, 2011, **133**, 10512. (b) A. Kondo, K. Maeda, *J. Solid State Chem.*, 2015, **221**, 126. (c) S. S. Nagarkar, A. K. Chaudhari, S. K. Ghosh, *Cryst. Growth Des.*, 2012, **12**, 572.
13. G. R. Desiraju, T. Steiner, *The Weak Hydrogen bond: In Structural Chemistry and Biology*, Oxford University Press, USA, **2001**.
14. (a) J. -R. Li, J. Sculley, H. -C. Zhou, *Chem. Rev.*, 2012, **112**, 869. (b) J. Duan, M. Higuchi, M. L. Foo, S. Horike, K. P. Rao, S. Kitagawa, *Inorg. Chem.*, 2013, **52**, 8244. (c) B. Mu, F. Li, Y. Huang, K. S. Walton, *J. Mater. Chem.*, 2012, **22**, 10172. (d) J. Wang, J. Luo, J. Zhao, D. -S. Li, G. Li, Q. Hui, Y. Liu, *Cryst. Growth Des.*, 2014, **14**, 2375.





The porous structure of the Ln(III) coordination polymer constructed with the conformationally flexible ligand was modulated by the guest solvent.